Intraseasonal variations in the surface layer heat balance of the central equatorial Indian Ocean: The importance of zonal advection and vertical mixing

M. J. McPhaden[1] and G. R. Foltz[2]

Received 28 March 2013; revised 2 May 2013; accepted 3 May 2013; published 6 June 2013.

[1] We examine the ocean mixed layer response to intraseasonal atmospheric forcing using moored time series data in the central equatorial Indian Ocean for October 2004 to March 2005, a period coincident with two active phases of the Madden-Julian Oscillation (MJO). Both MJO events were accompanied by a sea surface temperature decrease that was partially the consequence of reduced net surface heat flux. In addition, during the first event in October–November 2004, advection by an enhanced Wyrtki Jet contributed substantial cooling, while during the second event in December 2004 to January 2005, vertical processes, most likely related to entrainment mixing, were pronounced. Heavy rainfall at the mooring location during the first event may have contributed to the formation of a 30–40 m thick barrier layer that limited turbulent vertical transfers between the mixed layer and the thermocline. There was no barrier layer present during the second event, which presumably allowed for much freer vertical turbulent exchanges. **Citation:** McPhaden, M. J., and G. R. Foltz (2013), Intraseasonal variations in the surface layer heat balance of the central equatorial Indian Ocean: The importance of zonal advection and vertical mixing, *Geophys. Res. Lett.*, *40*, 2737–2741, doi:10.1002/grl.50536.

1. Introduction

[2] The Madden-Julian Oscillation (MJO) is the dominant form of intraseasonal variability in the tropical atmosphere, originating over the Indian Ocean with a periodicity of roughly 30–90 days [*Zhang*, 2005]. It has far reaching impacts on weather and climate, affecting Asian and Australian monsoon rainfall, rainfall along the west coast of the U.S., tropical storm formation, the evolution of El Niño events, and the North Atlantic Oscillation [*Zhang*, 2005; *Cassou*, 2008]. Interaction with ocean surface mixed layer temperatures may help to organize and amplify MJO variability and enhance its predictability [*Flatau et al*, 1997; *Fu et al*, 2007]. Thus, it is important to understand the processes involved in controlling the surface layer heat balance on intraseasonal time scales in the equatorial Indian Ocean where the MJO is spawned.

[3] Early studies identified interactions between intraseasonal fluctuations in the ocean surface layer and the overlying atmosphere in the Indian Ocean using a variety of in situ and satellite data [e.g., *McPhaden*, 1982a; *Sengupta et al*, 2001; *Vecchi and Harrison*, 2002]. With the advent of the Indian Ocean Observing System and the Research Moored Array for African-Asian-Australian Monsoon Analysis and Prediction (RAMA) [*McPhaden et al*, 2009] in the mid-2000s, comprehensive empirical analyses of the surface layer heat balance on intraseasonal time scales became possible with well-resolved (in time and depth) ocean measurements and high-quality surface heat flux data. For example, using RAMA mooring and other data at 8°S, 67°E in the shallow Seychelles-Chagos Thermocline Ridge region of the Indian Ocean during late 2007 to early 2008, *Vialard et al* [2008] concluded that "…atmospheric fluxes dominated the upper ocean heat balance at the MJO timescale…" Analysis of RAMA data in the central Bay of Bengal at 8°N, 90°E on the other hand indicates that the surface layer heat balance there is affected by both surface heat fluxes and vertical heat fluxes at the base of mixed layer on intraseasonal time scales [*Girishkumar et al*., 2013]. The Bay of Bengal is a region of strong salinity stratification where thick salt-stratified barrier layers support subsurface temperature inversions because of substantial river runoff and heavy rainfall. Thus, vertical turbulent fluxes at the base of the mixed layer can lead to mixed layer warming rather than cooling in the presence of temperature inversions. *Drushka et al* [2012] used Argo data and various surface flux data products to infer that surface heat fluxes dominated the surface layer temperature balance on intraseasonal time scales in the Indian Ocean but, because of the coarse 10 day temporal resolution of the Argo data and the uncertainties amongst the various flux data products, other processes could not be discerned with reliability.

[4] Recently, a major international field program called the Cooperative Indian Ocean experiment on intraseasonal variability (CINDY) was carried out from October 2011 to March 2012 to study the onset and development of the MJO. This program, together with a coordinated U.S. contribution called the Dynamics of the Madden Julian Oscillation (DYNAMO), involved intensive ship, aircraft, mooring, glider, and many other kinds of oceanic and atmospheric measurements [*Yoneyama et al*, 2013]. CINDY/DYNAMO was designed to test three hypotheses, one of which was specific to oceanic variability: "The barrier-layer, wind- and shear-driven mixing, shallow thermocline, and mixing-layer entrainment all play essential roles in MJO initiation over the Indian Ocean by controlling the upper ocean heat content and sea surface temperature, and thereby surface flux feedback." The field program was centered near the heavily instrumented RAMA mooring at 0°, 80.5°E in part to provide historical context for interpreting measurements from the shorter, more intensively sampled CINDY/DYNAMO period.

Additional supporting information may be found in the online version of this article.

[1]NOAA/Pacific Marine Environmental Laboratory, Seattle, Washington, USA.
[2]NOAA/Atlantic Oceanographic and Meteorological Laboratory, Miami, Florida, USA.

Corresponding author: M. J. McPhaden, NOAA/Pacific Marine Environmental Laboratory, 7600 Sand Point Way NE, Seattle, WA 98115, USA. (Michael.J.Mcphaden@noaa.gov)

0094-8276/13/10.1002/grl.50536

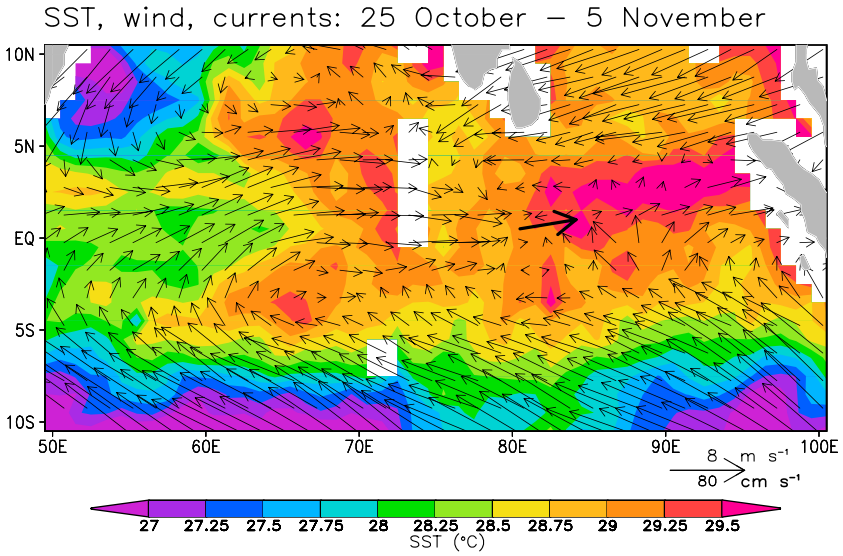

Figure 1. Twelve day average AMSR-E SST and Quikscat surface wind vectors for 25 October to 5 November 2004. Overplotted in bold is the corresponding 12 day average current velocity at 20 m depth from the RAMA mooring, with the tail of the arrow located at the mooring site. Note that SST increases to the east along the equator so that zonal advection leads to cooling at the mooring location for this period.

[5] The purpose of this study it to examine the surface layer heat balance using data principally from the RAMA mooring at 0°, 80.5°E. Unlike some other locations in RAMA, a detailed diagnosis of the intraseasonal mixed layer temperature balance at 0°, 80.5°E has not been carried out with moored time series data for any period in the data record. We thus focus on the initial RAMA mooring deployment at this location for 23 October 2004 to 20 March 2005, after which the mooring was vandalized and eventually lost. It is instructive to examine data from the initial deployment at this location because two MJO events occurred which, as we will see, resulted in two very different ocean mixed layer responses. Also, this period coincided with the development of a weak El Niño, which appears to have been largely forced by episodic surface westerly winds in the western Pacific associated with the MJO [*Lyon and Barnston*, 2005; *McPhaden et al*, 2006]. The variations we describe occurred during the same calendar months as CINDY/DYNAMO but in different years, providing a valuable comparative analysis for CINDY/DYNAMO studies presently underway.

2. Data and Methods

[6] For sea surface temperature (SST), we use an optimally interpolated Advanced Microwave Scanning Radiometer for Earth Observing System (AMSR-E) product with 3 day temporal resolution. For surface wind data, we use daily averages from the QuickScat scatterometer available from the Center for Satellite Exploitation and Research (CERSAT). The SST data set is available on a regular 0.25° grid and winds are on a 0.5° grid.

[7] We use daily average data from 23 October 2004 to 20 March 2005 collected from a NOAA Pacific Marine Environmental Laboratory (PMEL) next generation Autonomous Temperature Line Acquisition System (ATLAS) mooring deployed at 0°, 80.5°E (Figure 1). Measurements include sea surface and subsurface temperature and salinity, air temperature, relative humidity, wind velocity, shortwave and longwave radiation, and rainfall. The mooring measured ocean temperature at 1 m (nominally designated SST), 5 m, 10 m, 13 m, 20 m, 40 m, 43 m, 60 m, 80 m, 100 m, 120 m, 140 m, 180 m, 300 m, and 500 m. Conductivity (for salinity calculations) was measured at 1 m, 5 m, 10 m, 20 m, 40 m, 60 m, 100 m, and 140 m. Meteorological measurements were made 3–4 m above sea level and ocean currents were measured at 20 m depth.

[8] As in *Vialard et al* [2008], we consider a simplified version of the surface layer heat balance

$$\rho c_p h \partial T/\partial t = Q_0 - \rho c_p h[u\partial T/\partial x + v\partial T/\partial y] + R \qquad (1)$$

where T is the average mixed layer temperature, u and v are mixed layer currents, $\partial T/\partial x$ and $\partial T/\partial y$ are horizontal temperature gradients, h is the mixed layer depth (MLD), ρc_p is the volumetric heat capacity of seawater, and R is a residual. The left-hand side of (1) represents the change in mixed layer heat storage, Q_0 is the net surface heat flux, and $u\partial T/\partial x$ and $v\partial T/\partial y$ are horizontal advection terms, all of which can be directly estimated using mooring data in combination with satellite data. The net surface heat flux is the sum of latent and sensible heat flux, shortwave and longwave radiation, and the penetrative component of shortwave radiation through the base of the mixed layer:

$$Q_0 = Q_L + Q_S + Q_{SW} + Q_{LW} + Q_{pen} \qquad (2)$$

[9] We computed horizontal advection using the currents measured at 20 m from the mooring and centered differences of SST over 3° longitude and 3° latitude from the AMSR-E SST product. The residual R includes the effects of subsurface vertical processes that we cannot estimate directly such as upwelling, entrainment and vertical turbulent heat flux at the base of the mixed layer, plus any errors in the computation of other terms in (1).

[10] We estimate h as the depth at which the density is 0.15 kg m^{-3} greater than at 5 m [*Foltz et al*, 2010], where 5 m is chosen as a reference depth to avoid biases from sharp vertical density gradients in the shallow diurnal mixed layer. Mixed layer temperature is computed as the average temperature

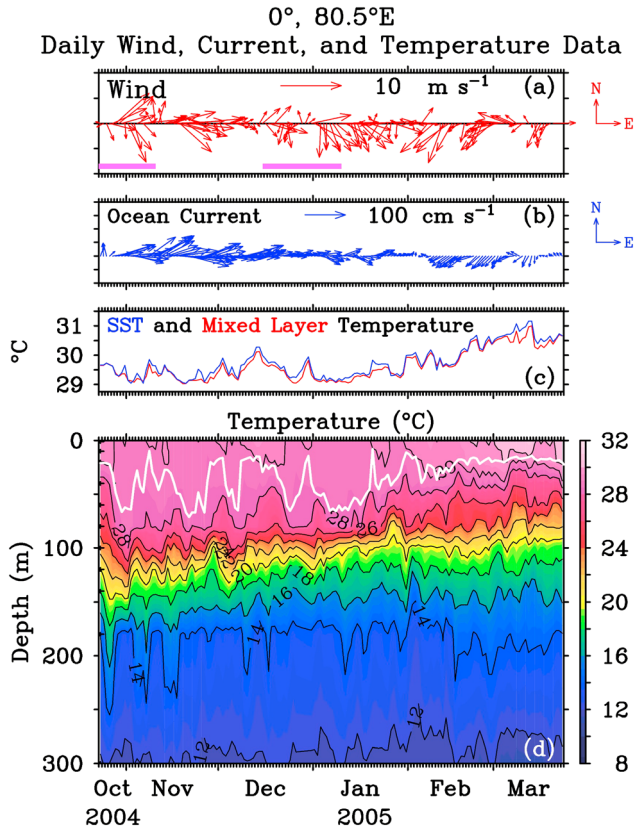

Figure 2. Daily time series of (a) wind vectors, (b) currents at 20 m depth, (c) SST (blue) and mixed layer temperature (red), and (d) upper ocean temperature from the RAMA mooring at 0°, 80.5°E. Overplotted on Figure 2d is the mixed layer depth. Pink horizontal lines in Figure 2a indicate active phases of the MJO according to Figure S2.

over h using the mooring data. It is highly correlated with and nearly identical to SST (Figure 2c). Isothermal layer depth (ILD) is calculated using the temperature equivalent of a 0.15 kg m^{-3} density increase from 5 m. Barrier layer thickness (BLT) is defined as the difference of ILD − MLD.

[11] The conductivity sensor failed at 20 m so that salinity could not be computed directly at this depth. We filled this gap using linear interpolation from neighboring depths. To ensure our MLD depth and BLT estimates are reasonable given the relatively coarse vertical resolution for density computations, we compared these estimates to those obtained from six conductivity-temperature-depth profiles with 1 m vertical resolution within 170 km of the buoy during the deployment cruise. We estimate errors in MLD and ILD of typically ~7–8 m, giving errors in barrier layer thickness of about 10 m [see *Foltz and McPhaden*, 2009]. As discussed below, the differences in MLD and BLT are small relative to the variations we observe so that the missing salinity data do not introduce great uncertainty into our results.

[12] We estimated latent and sensible heat fluxes using mooring data and the Coupled Ocean-Atmosphere Response Experiment (COARE) version 3.0 bulk flux algorithm [*Fairall et al.*, 2003]. Net surface shortwave radiation (Q_{SW}) was computed assuming an albedo of 6% for downward shortwave flux observations made on the mooring. We estimated the amount of Q_{SW} that penetrates below the mixed layer using monthly climatological Sea-viewing Wide Field-of-view Sensor (SeaWiFS) chlorophyll-a concentrations following the method developed by *Morel and Antoine* [1994] and using the coefficients provided by *Sweeney et al.* [2005]. Net longwave radiation was computed from measured downwelling longwave radiation adjusted for black body radiation from the sea surface. Surface heat fluxes are defined as positive when they heat the mixed layer (Figure S1 in the auxiliary material).

3. Results

[13] The moored buoy time series at 0°, 80.5°E exhibit substantial seasonal and intraseasonal variations during October 2004 to March 2005. Seasonally, the beginning of the record is characterized by strong westerly monsoon transition winds in October to December 2004, giving way to northeast monsoon winds by February–March 2005 (Figure 2a). The zonal surface layer currents accelerate quickly in the direction of the winds, with development of a strong eastward Wyrtki Jet in late 2004 followed in February–March by a westward Northeast Monsoon Current. SST and mixed layer temperatures rise through the boreal winter, which is part of the normal seasonal cycle in the central equatorial Indian Ocean due to the maximum in net surface heat flux at this time of year [*McPhaden*, 1982b]. Weakening and shoaling of the thermocline in February–March 2005 are associated with the development of a transient eastward equatorial undercurrent, which normally develops at this time of year in response to northeast monsoon wind forcing [*Nagura and McPhaden*, 2008].

[14] Superimposed on these seasonal variations are considerable intraseasonal fluctuations, especially noticeable during the period October 2004 to January 2005. Evident during this time are weekly changes of nearly 10 m s^{-1} in wind speed, 50 cm s^{-1} in zonal current, 1°C in SST, and 50 m in mixed layer depth. According to NOAA's Climate Prediction Center, two episodes of enhanced MJO convective activity occurred during this time, one in late October to early November 2004 and a second in mid-December to early January 2005 (Figure S2). Other periods of convection and disturbed weather occurred as well at this location, though not necessarily related to the MJO (for example in mid-November 2004 and mid-February 2005).

[15] Various terms in the mixed layer temperature balance (Figure 3) illustrate the processes controlling SST during this period. Q_{SW} and Q_L dominate surface heat flux variations as is typical in the tropics, with a substantial amount of Q_{SW} (up to 60 W m^{-2} at times) penetrating through the base of the mixed layer. Q_L varies mostly in response to wind speed variations at this location because of the high overall mean SSTs (Figure S1), similar to what happens on MJO time scales in the western Pacific warm pool [*Zhang and McPhaden*, 1995]. Thus, local minima in Q_L occur in late October to early November and mid-December to early January associated with high MJO-related surface wind speeds, coincident with local minima in Q_{SW} associated with MJO convective cloudiness (Figures 3a and S2). Other minima in Q_L and Q_{SW} in mid-November and mid-February are not related to the MJO.

[16] The net surface heat flux (Figure 3b) is almost always positive, ranging from ~100 W m^{-2} in late November to −50 W m^{-2} for a brief period in mid-November. Surface flux heating of the mixed layer is near zero during the active phase of the MJO in late October to early November and approximately 50 W m^{-2} during the active phase between

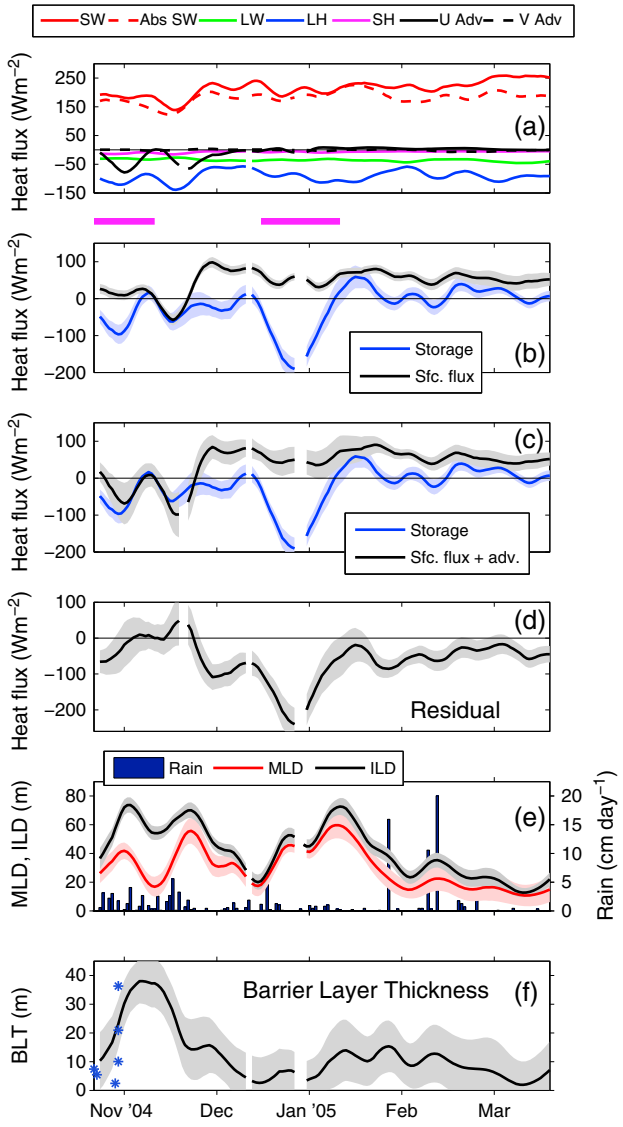

Figure 3. Time series of (a) mixed layer heat budget components, including shortwave radiation absorbed by the mixed layer (Abs SW) which takes into account the penetrative component of radiation, (b) net surface heat flux and mixed layer heat storage rate, (c) as in Figure 3b but including horizontal advection, (d) residual of directly computed heat budget terms, (e) mixed layer depth (MLD), isothermal layer depth (ILD) and rainfall, and (f) barrier layer thickness (BLT). All time series have been smoothed with a 15 day running mean filter. Shadings in Figures 3b–3f indicate 90% confidence levels calculated using the methodology of *Foltz and McPhaden* [2009]. Pink horizontal lines between Figures 3a and 3b indicate active phases of the MJO according to Figure S2. Asterisks in Figure 3f indicate BLT computed from individual conductivity-temperature-depth casts during the mooring deployment cruise.

mid-December and early January. A significant imbalance occurs in the mixed layer heat balance though, considering only these surface flux variations in relation to heat storage (Figure 3b).

[17] Taking into account zonal advection linked to the strong wind driven eastward flows associated with the Wyrtki Jet generally improves agreement between the left- and right-hand sides of (1) from late October to mid-November (Figure 3c). During this time, zonal advection tends to cool the mixed layer by 50–100 W m^{-2}. Thus, on average, cooling from the residual (Figure 3d) is much smaller from late October to mid-November (0–50Wm^{-2}), a period that includes the first active phase of the MJO, than for mid-December to early January (100–200Wm^{-2}), which coincides with the second active phase of the MJO.

[18] An important distinction between these two periods is that the mixed layer and isothermal layer depths are nearly identical from mid-December to early January during the second MJO event whereas, except in late October, the MLD is 30–40 m shallower than the ILD over much of the first MJO event (Figure 3e). We surmise that the thick barrier layer inhibits turbulent heat transfers between the mixed layer and thermocline during most of the first event but the absence of a thick barrier during the second event allows much freer turbulent exchange between the mixed layer and the thermocline (Figure 3f). The mixed layer deepens by ~50 m over the course of the second MJO from mid-December to early January (Figure 3e) while the depth of the thermocline changes little (Figure 2d), suggesting that there is significant turbulent entrainment that contributes to the observed mixed layer cooling over this time. A complete explanation for why these distinctions in BLT and vertical turbulent mixing occur during the two MJO events requires a thorough examination of sources and sinks for the turbulence energy budget of the mixed layer. Such an analysis is beyond the scope of this paper, though we note that the rainfall is heavier and more frequent during the first MJO event (Figure 3e). The buoyancy flux associated with these higher rainfall totals may have been sufficient to overcome sources of wind-driven or current shear-driven turbulence generation to favor the formation of a thick barrier layer then.

4. Summary and Conclusions

[19] In this study we have examined the ocean mixed layer response to intraseasonal atmospheric forcing, with emphasis on the MJO, using RAMA moored time series data for October 2004 to March 2005. This period coincided with two distinct active phases of the MJO, one from late October to early November 2004 and a second from mid-December 2004 to early January 2005. Both MJO events were accompanied by a decrease in SST that was in part the consequence of reduced net surface heat flux. Changes in net surface heat flux resulted from coincident increases in latent heat loss from the ocean associated with strong MJO-related winds and decreases in shortwave radiation associated with enhanced MJO-related cloudiness. In combination, these effects resulted in surface heat fluxes during active phases of the MJO that were 50–100 W m^{-2} lower than during periods of suppressed convection such as between mid-November and mid-December 2004.

[20] However, surface heat fluxes alone do not account for the changes in observed mixed layer heat storage. During the first MJO event, zonal advection by an enhanced Wyrtki Jet contributed an additional cooling of 50–100 W m^{-2} while during the second MJO event vertical processes, most likely related to entrainment mixing, cooled the mixed layer at a rate of up to 200 W m^{-2}. Rainfall was heavier and more frequent at the mooring location during the first event, which may have contributed to the formation of a 30–40 m thick

barrier layer that limited turbulent vertical transfers between the mixed layer and the thermocline. There was no barrier layer present during the second event, which allowed for much freer vertical exchange with the thermocline.

[21] Thus, MJO forcing in the central equatorial Indian Ocean can lead to very different responses in the ocean mixed layer. Surface heat flux forcing (mainly through variations in latent heat flux and shortwave radiation) is important, but the ocean mixed layer is far more complicated than a simple slab that responds only to surface heat fluxes. The potential for very strong wind-forced zonal current advection and vigorous vertical mixing must be considered as well. The details of how the ocean responds to MJO forcing will depend on the details of individual MJO events, the time of year, and oceanic initial conditions. Also, because the MJO evolves in both space and time, it is likely that the oceanic response to MJO forcing will not be uniform across the Indian Ocean basin. Hence, to accurately simulate intraseasonal SST variations in coupled models, it will be necessary to properly represent the range of mixed layer processes that can affect the storage of heat in the mixed layer.

[22] **Acknowledgments.** This work was supported by NOAA. We thank Ren-Chieh Lien of the University of Washington Applied Physics Laboratory and an anonymous reviewer for helpful comments on an earlier version of this manuscript and Dai McClurg of PMEL for assistance with graphics. PMEL contribution 4007.

[23] The Editor thanks Ren-Chieh Lien and an anonymous reviewer for their assistance in evaluating this paper.

References

Cassou, C. (2008), Intraseasonal interaction between the Madden–Julian Oscillation and the North Atlantic Oscillation, *Nature*, *455*, 523–527.

Drushka, K., J. Sprintall, S. T. Gille, and S. Wijffels (2012), In situ observations of Madden–Julian Oscillation mixed layer dynamics in the Indian and western Pacific Oceans, *J. Clim.*, *25*, 2306–2328.

Fairall, C. W., E. F. Bradley, J. E. Hare, A. A. Grachev, and J. B. Edson (2003), Bulk parameterization of air-sea fluxes: Updates and verification for the COARE algorithm, *J. Clim.*, *16*, 571–591.

Flatau, M., P. J. Flatau, P. Phoebus, and P. P. Niiler (1997), The feedback between equatorial convection and local radiative and evaporative processes: The implications for intraseasonal oscillations, *J. Atmos. Sci.*, *54*, 2373–2386.

Foltz, G. R., and M. J. McPhaden (2009), Impact of barrier layer thickness on SST in the central tropical North Atlantic, *J. Clim.*, *22*, 285–299.

Foltz, G. R., J. Vialard, P. Kumar, and M. J. McPhaden (2010), Seasonal mixed layer heat balance of the southwestern tropical Indian Ocean, *J. Climate*, *23*, 947–965.

Fu, X., B. Wang, D. E. Waliser, and L. Tao (2007), Impact of atmosphere–ocean coupling on the predictability of monsoon intraseasonal oscillations, *J. Atmos. Sci.*, *64*, 157–174.

Girishkumar, M. S., M. Ravichandran, and M. J. McPhaden (2013), Temperature inversions and their influence on the mixed layer heat budget during the winters of 2006–07 and 2007–08 in the Bay of Bengal, *J. Geophys. Res.*, doi:10.1002/jgrc.20192, in press.

Lyon, B., and A. G. Barnston (2005), *The Evolution of the Weak 2004–2005 El Niño, U.S. CLIVAR Variations*, 3 (2), pp. 1–4, U. S. Clim. Variability and Predict. Office, Washington, D. C.

McPhaden, M. J. (1982a), Variability in the central equatorial Indian Ocean, part I: Ocean dynamics, *J. Mar. Res.*, *40*, 157–176.

McPhaden, M. J. (1982b), Variability in the central equatorial Indian Ocean, part II: Oceanic heat and turbulent energy balance, *J. Mar. Res.*, *40*, 403–419.

McPhaden, M. J., X. Zhang, H. H. Hendon, and M. C. Wheeler (2006), Large scale dynamics and MJO forcing of ENSO variability, *Geophys. Res. Lett.*, *33*(16), L16702, doi:10.1029/2006GL026786.

McPhaden, M. J., G. Meyers, K. Ando, Y. Masumoto, V. S. N. Murty, M. Ravichandran, F. Syamsudin, J. Vialard, L. Yu, and W. Yu (2009), RAMA: The Research Moored Array for African-Asian-Australian Monsoon Analysis and Prediction, *Bull. Am. Meteorol. Soc.*, *90*, 459–480.

Morel, A., and D. Antoine (1994), Heating rate within the upper ocean in relation to its bio-optical state, *J. Phys. Oceanogr.*, *24*, 1652–1665.

Nagura, M., and M. J. McPhaden (2008), The dynamics of zonal current variations in the central equatorial Indian Ocean. *Geophys. Res. Lett.*, *35*, K23603, doi:10.1029/2008GL035961.

Sengupta, D., B. N. Goswami, and R. Senan (2001), Coherent intraseasonal oscillations of the ocean and atmosphere during the Asian summer monsoon, *Geophys. Res. Lett.*, *28*(21), 4127.

Sweeney, C., A. Gnanadesikan, S. Griffies, M. Harrison, A. Rosati, and B. Samuels (2005), Impacts of shortwave penetration depth on large-scale ocean circulation heat transport, *J. Phys. Oceanogr.*, *35*, 1103–1119.

Vecchi, G. A., and D. E. Harrison (2002), Monsoon breaks and subseasonal sea surface temperature variability in the Bay of Bengal, *J. Climate*, *15*, 1485–1493.

Vialard, J., G. R. Foltz, M. J. McPhaden, J. P. Duvel, and C. de Boyer Montégut, (2008), Strong Indian Ocean sea surface temperature signals associated with the Madden-Julian Oscillation in late 2007 and early 2008, *Geophys. Res. Lett.*, *35*, L19608, doi:10.1029/2008GL035238.

Yoneyama, K., C. Zhang, and C. N. Long (2013), Tracking pulses of the Madden-Julian Oscillation, *Bull. Am. Meteor. Soc.*, in press.

Zhang, C. (2005), Madden-Julian Oscillation, *Rev. Geophys.*, *43*, RG2003, doi:10.1029/2004RG000158.

Zhang, G. J., and M. J. McPhaden (1995), On the relationship between sea surface temperature and latent heat flux in the equatorial Pacific, *J. Clim.*, *8*, 589–605.